

Low-temperature electrical transport in bilayer manganite $\text{La}_{1.2}\text{Sr}_{1.8}\text{Mn}_2\text{O}_7$

C. L. Zhang, X. J. Chen, and C. C. Almasan

Department of Physics, Kent State University, Kent OH 44242, USA

J. S. Gardner

Chalk River Laboratory, Chalk River ON K0J 1PO, Canada

J. L. Sarrao

Los Alamos National Laboratory, Los Alamos, NM 87545, USA

(Dated: Received 17 October 2001)

The temperature T and magnetic field H dependence of anisotropic in-plane ρ_{ab} and out-of-plane ρ_c resistivities have been investigated in single crystals of the bilayer manganite $\text{La}_{1.2}\text{Sr}_{1.8}\text{Mn}_2\text{O}_7$. Below the Curie transition temperature $T_c = 125$ K, ρ_{ab} and ρ_c display almost the same temperature dependence with an up-turn around 50 K. In the metallic regime ($50 \text{ K} \leq T \leq 110$ K), both $\rho_{ab}(T)$ and $\rho_c(T)$ follow a $T^{9/2}$ dependence, consistent with the two-magnon scattering. We found that the value of the proportionality coefficient B_{ab}^{fit} and the ratio of the exchange interaction J_{ab}/J_c obtained by fitting the data are in excellent agreement with the calculated B_{ab} based on the two-magnon model and J_{ab}/J_c deduced from neutron scattering, respectively. This provides further support for this scattering mechanism. At even lower T , in the non-metallic regime ($T < 50$ K), both the in-plane σ_{ab} and out-of-plane σ_c conductivities obey a $T^{1/2}$ dependence, consistent with weak localization effects. Hence, this demonstrates the three-dimensional metallic nature of the bilayer manganite $\text{La}_{1.2}\text{Sr}_{1.8}\text{Mn}_2\text{O}_7$ at $T < T_c$.

PACS numbers: 75.30.Vn, 72.15.-v, 72.10.-d

I. INTRODUCTION

There is growing interest in the low-temperature electrical transport phenomena of perovskite manganites in order to elucidate the microscopic origin of the colossal magnetoresistance (CMR) effect.^{1,2,3,4,5,6} Recent studies on single crystals of the three-dimensional 3D pseudocubic compounds $R_{1-x}A_x\text{MnO}_3$ (R is a trivalent rare-earth ion and A is a divalent alkaline-earth ion) show a T^2 dependence of the resistivity,^{2,3,4} which has been interpreted as either electron-electron^{3,4} or one-magnon² scattering. However, low-temperature resistivity measurements of epitaxial thin films of $\text{La}_{1-x}\text{Ca}_x\text{MnO}_3$ provide support for the presence of small-polaron conduction in the ferromagnetic (FM) state.^{5,6} In the same system, a $T^{9/2}$ term attributed to electron-magnon scattering was also found in the T dependence of resistivity at low-temperatures.^{1,6} Therefore, the low-temperature electrical transport mechanism of manganites remains controversial and is far from being fully understood.

The bilayer manganite $\text{La}_{2-2x}\text{Sr}_{1+2x}\text{Mn}_2\text{O}_7$ has proven to be a fruitful system for understanding the CMR and has become the focus of many recent investigations.^{7,8} This is an ideal system for the study of the low-temperature conduction mechanism. Its reduced dimensionality gives rise to anisotropic characteristics of charge transport and magnetic properties and also enhances the CMR effect near the magnetic transition temperature, although at the cost of reducing it to about 100 K.⁷ The magnetic structure of heavily doped bilayer compounds always shows the coexistence of FM and antiferromagnetic (AFM) correlations.^{9,10,11,12} The

magnetic correlations are predominantly FM within the two-dimensional MnO_2 layers, while the magnetic coupling between the MnO_2 layers changes from FM for $x \leq 0.4$ to canted AFM for $x > 0.4$. The interplay between FM double exchange and AFM superexchange interactions between Mn ions in these compounds becomes more subtle and is expected to be responsible for the unusual transport properties observed in the bilayer manganites. For examples, (i) an up-turn in the resistivity at low temperatures is generally observed for the $x = 0.30$,¹⁵ 0.35,¹⁶ 0.38,¹⁵ and 0.47,^{13,14} samples; (ii) despite the anisotropic crystal structure,¹⁷ ρ_{ab} and ρ_c of the $x = 0.38$ compound display virtually identical temperature dependences at low-temperatures, indicating the same conduction mechanism in both ab and c directions.¹⁵

A lot of effort has been devoted to understanding the low-temperature electrical transport properties of bilayer manganites. Okuda, Kimura, and Tokura¹⁶ found that the in-plane conductivity σ_{ab} of $x = 0.35$ single crystals is almost proportional to $T^{1/2}$ for $T < 4$ K, indicating weak localization. This square-root temperature dependence of σ_{ab} was also observed in the $x = 0.40$ samples.¹⁴ Recently, Abrikosov, based on the theory of quantum interference, has shown that $\sigma_{ab}(T)$ and $\sigma_c(T)$ should be isotropic and proportional to $\tau_\varphi^{-1/2}$ (the phase coherence destruction probability $\tau_\varphi^{-1} \propto T$ for the 3D conduction) in the 3D (low-temperature) regime.¹⁸ It is, therefore, desirable from the experimental point of view to determine $\sigma_c(T)$ of bilayer manganites and, hence, to establish which scattering mechanism is mainly responsible for the low-temperature transport properties of this system. An important question is also whether there is

any common conduction mechanism responsible for the low-temperature electrical transport in both the infinite-layer and bilayer manganites.

In this paper, we address the above issues through resistivity measurements on $\text{La}_{1.2}\text{Sr}_{1.8}\text{Mn}_2\text{O}_7$ single crystals, performed at low temperatures and in magnetic fields applied parallel to the ab plane. The anisotropic resistivities $\rho_{ab}(T)$ and $\rho_c(T)$ are proportional to $T^{9/2}$ in the intermediate temperature regime below T_c . This points toward a two-magnon scattering mechanism responsible for the electrical dissipation in this T range. The validity of this scattering mechanism is further supported by the H dependence of the proportionality coefficients $B_{ab,c}^{fit}$ obtained by fitting the data and by the fact that the value of B_{ab}^{fit} and the ratio of the exchange interaction J_{ab}/J_c obtained by fitting the data are in excellent agreement with the calculated B_{ab} based on the two-magnon model and J_{ab}/J_c deduced from neutron scattering, respectively. At lower temperatures, in the non-metallic regime ($\partial\rho/\partial T < 0$), both anisotropic conductivities $\sigma_{ab}(T)$ and $\sigma_c(T)$ exhibit a $T^{1/2}$ dependence, a result of electron-electron correlations, which is consistent with the weak localization effect in a 3D disordered metal. The common mechanisms responsible for both the in-plane and out-of-plane electrical transport indicate the 3D metallic nature of the bilayer manganite $\text{La}_{1.2}\text{Sr}_{1.8}\text{Mn}_2\text{O}_7$ at $T < T_c$.

II. EXPERIMENTAL DETAILS

Single crystals of $\text{La}_{1.2}\text{Sr}_{1.8}\text{Mn}_2\text{O}_7$ were grown from sintered rods of the same nominal composition by the floating zone method using a mirror furnace, as described in detail elsewhere.¹⁹ Plate-shaped crystals were separated mechanically from the bar. X-ray diffraction confirmed that the surfaces of the plates are parallel to the crystallographic ab plane. The crystal chosen for systematic transport measurements had mirror surfaces on both faces. We determined ρ_{ab} and ρ_c as functions of temperature T ($1.9 \leq T \leq 400$ K) and magnetic field H ($0 \leq H \leq 14$ T) by performing multi-terminal transport measurements using the electrical contact configuration of the flux transformer, as described previously.^{20,21} The magnetic field H was applied parallel to the MnO_2 layers ($H \parallel ab$ plane).

III. RESULTS AND DISCUSSION

The T dependence of the magnetic susceptibility χ measured in a low H ($H = 10$ Oe) is shown in the inset to Fig. 1(b). The sample exhibits a paramagnetic (PM) - FM transition at the Curie transition temperature $T_c = 125$ K, which is consistent with previous reports.^{7,17} At $T < 50$ K, the susceptibility slightly decreases with decreasing T , in good agreement with recent reports.^{14,17} As typically seen in other studies,^{7,17,22} an additional

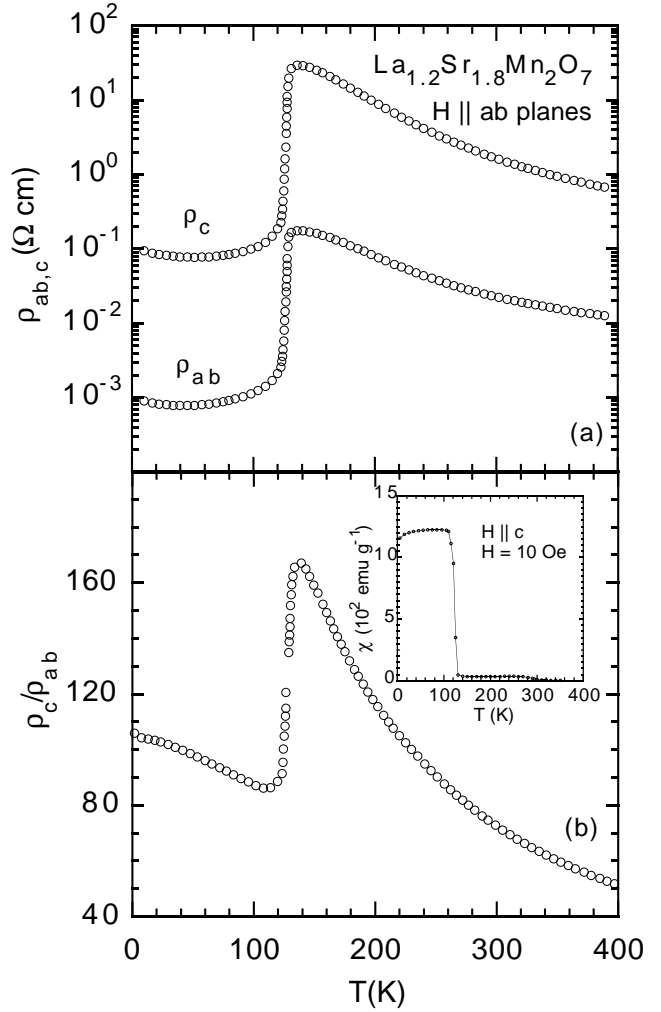


FIG. 1: Temperature T dependences of (a) in-plane ρ_{ab} and out-of-plane ρ_c resistivities measured in zero magnetic field and (b) anisotropy ρ_c/ρ_{ab} for $\text{La}_{1.2}\text{Sr}_{1.8}\text{Mn}_2\text{O}_7$. Inset: ac susceptibility χ as a function of temperature measured in a magnetic field $H = 10$ Oe.

transition appears around 290 K, most likely due to trace amounts of impurities²³ (intergrowth) that, however, represent only about 0.1 % of the volume fraction of the sample.²²

Figures 1(a) and 1(b) show the temperature profiles of ρ_{ab} and ρ_c , and of the anisotropy ρ_c/ρ_{ab} , respectively, measured in zero magnetic field. The metal-insulator transition takes place at $T_{MI} = 130$ K for both situations: current parallel (ρ_{ab}) and perpendicular (ρ_c) to the MnO_2 layers. The anisotropy ρ_c/ρ_{ab} increases with decreasing T , reaches its maximum value of 165 at T_{MI} , decreases abruptly just below T_c , and depends weakly on T for $T < T_c$ with an average value of ~ 90 , comparable to other measurements.^{7,13} We note that the values of both ρ_{ab} and ρ_c are, over the whole measured T range, appreciably smaller than those reported previously,⁷ attesting to the high quality of our single crystal.

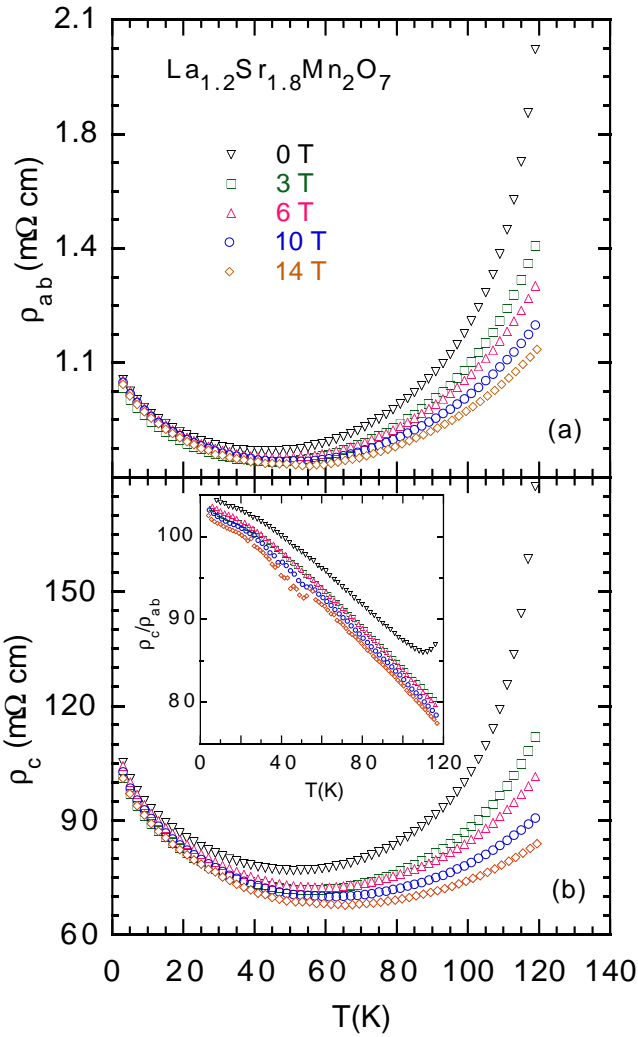


FIG. 2: Plot of (a) in-plane resistivity ρ_{ab} and (b) out-of-plane resistivity ρ_c vs temperature T for $\text{La}_{1.2}\text{Sr}_{1.8}\text{Mn}_2\text{O}_7$ measured in applied magnetic fields H up to 14 T. Inset: Anisotropy ρ_c/ρ_{ab} vs T in the temperature range from 2 to 120 K measured under various H .

The H and T dependences of ρ_{ab} and ρ_c are shown in Figs. 2(a) and 2(b), respectively, for the temperature range from 2 to 120 K. The characteristic negative magnetoresistivity in both ρ_{ab} and ρ_c is clearly seen over the whole T range. At the same time, ρ_c/ρ_{ab} has a weaker H dependence [see inset to Fig. 2(b)]. An interesting feature of $\rho_{ab}(T)$ and $\rho_c(T)$ is the appearance of a weak non-metallic behavior for $T < 50$ K in zero field, which shifts to higher temperatures with increasing magnetic field.

In the infinite-layer $\text{La}_{1-x}\text{Sr}_x\text{MnO}_3$ ($0.10 \leq x \leq 0.17$) samples, a similar low-temperature up-turn in resistivity has been identified with the vestiges of the structural O^* to O' transition in the FM phase.²⁴ Temperature-dependent neutron diffraction studies on $\text{La}_{1.2}\text{Sr}_{1.8}\text{Mn}_2\text{O}_7$ do not show any structural transition

occurring at low-temperatures.¹⁷ The up-turn in the resistivity of $\text{La}_{1.2}\text{Sr}_{1.8}\text{Mn}_2\text{O}_7$ at low temperatures is accompanied by a decrease of the ac susceptibility, which is related to the reentrant spin glass phase,¹⁴ an indication of a crossover from a FM to a canted state.²⁵ The canted structure at low temperatures comes from the competing interactions along the c -axis Mn-O-Mn bonds, *i.e.*, the AFM superexchange interaction between half-filled t_{2g} orbitals and the FM double-exchange interaction via e_g conduction electrons.²⁵

In ordinary FM metals, the contribution to resistance from the $s-d$ interaction is known to be proportional to T^2 at low temperatures.^{26,27} This T^2 dependence of resistivity has been generally observed in single crystals of $\text{La}_{1-x}\text{Sr}_x\text{MnO}_3$ ($x > 0.18$),³ $\text{La}_{1-x}\text{Ca}_x\text{MnO}_3$ ($x \geq 0.22$),⁴ and $\text{La}_{0.67}(\text{Pb},\text{Ca})_{0.33}\text{MnO}_3$,² and has been attributed to either electron-electron^{3,4} or one-magnon² scattering. However, our low-temperature resistivities data ($50 \text{ K} \leq T \leq 110 \text{ K}$) of $\text{La}_{1.2}\text{Sr}_{1.8}\text{Mn}_2\text{O}_7$ single crystals measured in various applied magnetic fields do not follow a T^2 dependence of the form $\rho(T) = \rho_0 + AT^2$. Therefore, the electron-electron scattering mechanism does not contribute to $\rho_{ab,c}(T)$. This indicates that the conduction mechanism in this bilayer manganite is different from that in the infinite-layer compounds. In fact, specific heat measurements on bilayer manganites¹⁶ show that their reduced dimensionality, compared to infinite-layer manganites, enhances the magnetic specific heat, but does not affect the electronic specific heat coefficient γ , indicating the presence of an anomalous carrier scattering process such as electron-phonon, electron-magnon, or a combination of them.

Polaronic transport has been recently shown to be a possible conduction mechanism in $\text{R}_{1-x}\text{A}_x\text{MnO}_3$ at $T < T_c$.^{5,6,28} Zhao *et al.*^{5,6} reported that the resistivity below 100 K in epitaxial thin films of $\text{La}_{1-x}\text{Ca}_x\text{MnO}_3$ ($x = 0.25$ and 0.4) grown on (100) LaAlO_3 substrates can be well fitted with $\rho = \rho_0 + E\omega_s/\sinh^2(\hbar\omega_s/2k_B T)$ (ω_s is the frequency of a soft optical mode), providing evidence for small-polaron metallic conduction in the FM state. We found that our resistivity data of $\text{La}_{1.2}\text{Sr}_{1.8}\text{Mn}_2\text{O}_7$ can not be adequately fitted with this expression. Presently, there is no experimental evidence for the presence of small polarons in the FM state of bilayer manganites. In fact, recent Raman scattering data on $\text{La}_{1.2}\text{Sr}_{1.8}\text{Mn}_2\text{O}_7$ single crystals suggest the formation of small polarons *only* at $T > T_c$.²⁹ Moreover, X-ray and neutron scattering measurements³⁰ on $\text{La}_{1.2}\text{Sr}_{1.8}\text{Mn}_2\text{O}_7$ directly demonstrate that the polarons disappear abruptly at the FM transition because of the sudden charge delocalization. On the other hand, the giant magnetothermal conductivity³¹ observed in $\text{La}_{1.2}\text{Sr}_{1.8}\text{Mn}_2\text{O}_7$ indicates that spin-fluctuation scattering or magnon contribution is dominant over other carrier scattering processes.

Kubo and Ohata³² calculated the low-temperature resistance produced by scattering of holes by spin waves, on the basis of an effective Hamiltonian for double exchange

in the spin wave approximation. They have found that the contribution from the two-magnon scattering process is proportional to $T^{9/2}$ and that the proportionality coefficient has, in the case of a simple parabolic band, the analytical expression given by

$$B = \frac{3\hbar R^6 k_F^5}{32\pi e^2 S^2} \left(\frac{m}{M}\right)^{9/2} \left(\frac{k_B}{E_F}\right)^{9/2} (2.52 + 0.0017 \frac{M}{m}). \quad (1)$$

Here R is the hopping distance of the e_g electrons in the in-plane or out-of-plane direction, S is the effective spin of a Mn ion, the Fermi energy E_F is measured from the band center, and M and m are the effective masses of a hole and a spin wave, respectively. In terms of the hole concentration per unit cell n , the effective hopping integral t^* , and the average spin stiffness D^* , the coefficient B can be rewritten as⁶

$$B = \frac{R\hbar}{48^2\pi^7 e^2 S^2} \frac{(6\pi^2 n)^{5/3}}{(0.5^{2/3} - n^{2/3})^{9/2}} \left(\frac{R^2 k_B}{D^*}\right)^{9/2} (2.52 + 0.0017 \frac{D^*}{R^2 t^*}). \quad (2)$$

Here the following simple relationships had been used: $Rk_F = (6\pi^2 n)^{1/3}$, $M/m = D^*/(R^2 t^*)$, and $E_F = t^*(6\pi^2)^{2/3}(0.5^{2/3} - n^{2/3})$.

To reveal the two-magnon scattering nature of the resistivity in $\text{La}_{1.2}\text{Sr}_{1.8}\text{Mn}_2\text{O}_7$, we plot in Figs. 3(a) and 3(b) the measured $\rho_{ab}(T)$ and $\rho_c(T)$, respectively, along with the fits of these data with $\rho(T) = \rho_0 + BT^{9/2}$. Both $\rho_{ab}(T)$ and $\rho_c(T)$ follow remarkably well a $T^{9/2}$ dependence (solid lines in the figures) in the T range of 50 to 110 K for different applied magnetic fields. The fitting parameters for $\rho_{ab}(T)$ and $\rho_c(T)$ measured in zero H are $B_{ab}^{fit} = 4.04 \times 10^{-13} \Omega \text{ cm}/\text{K}^{9/2}$ and $B_c^{fit} = 2.83 \times 10^{-11} \Omega \text{ cm}/\text{K}^{9/2}$, respectively.

We determine next the zero-field value of B_{ab} from Eq. (2) and compare it with the value of the corresponding fitting parameter. In $\text{La}_{1.2}\text{Sr}_{1.8}\text{Mn}_2\text{O}_7$, the hole concentration $n \equiv x = 0.40$, the in-plane hopping distance is the Mn-Mn distance $R_{ab} = 3.87 \text{\AA}$,¹⁷ the magnitude of the effective spin is $S = 1.8$,³³ the effective stiffness constant $D_{ab}^* = 151 \text{ meV \AA}^2$ based on recent neutron scattering measurements,³⁴ and $t^* = 40 \text{ meV}$ as estimated from the measured effective plasma frequency.⁶ With these values for different physical quantities, Eq. (2) gives $B_{ab} = 1.01 \times 10^{-13} \Omega \text{ cm}/\text{K}^{9/2}$. This value of B_{ab} has the same order of magnitude as the fitting parameter B_{ab}^{fit} , showing that the two-magnon scattering can account for the T dependence of resistivity of $\text{La}_{1.2}\text{Sr}_{1.8}\text{Mn}_2\text{O}_7$ in the metallic range of temperatures.

In a conventional Heisenberg system, the spin-wave stiffness D scales with the strength of the magnetic exchange coupling J and can be expressed as $D = JSR^2$.³⁵ Since $0.0017D^*/R^2t^* \ll 2.52$, one can ignore this term from Eq. (2). Hence, one obtains the following expression for the ratio of the in-plane J_{ab} and interlayer J_c exchange interactions:

$$\frac{J_{ab}}{J_c} = \left(\frac{B_c}{B_{ab}} \frac{R_{ab}}{R_c}\right)^{2/9}. \quad (3)$$

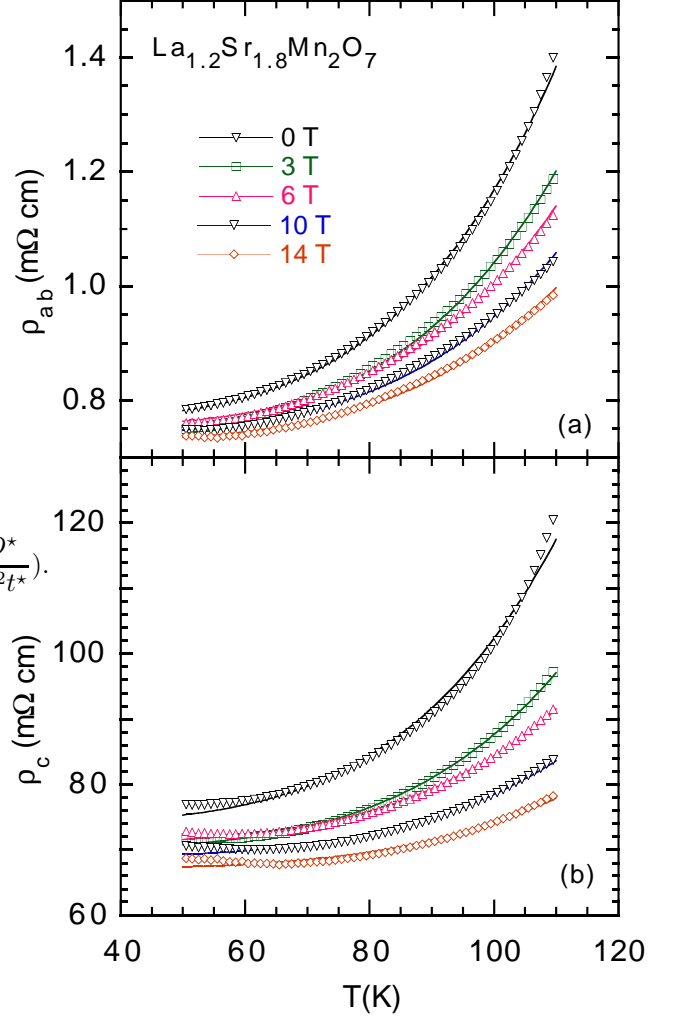


FIG. 3: (a) In-plane resistivity ρ_{ab} and (b) out-of-plane resistivity ρ_c vs temperature T for $\text{La}_{1.2}\text{Sr}_{1.8}\text{Mn}_2\text{O}_7$ measured under various applied magnetic fields H . The solid lines are fits of the data with a $T^{9/2}$ dependence.

With the values of B_{ab} and B_c obtained from the fitting, the hopping distance R_{ab} given above, and the out-of-plane hopping distance as the Mn-Mn distance between the MnO_2 layers $R_c = 3.88 \text{\AA}$,¹⁷ the above equation gives $J_{ab}/J_c = 2.6$. This value is in excellent agreement with the value of 2.8 determined from inelastic neutron scattering measurements on $\text{La}_{1.2}\text{Sr}_{1.8}\text{Mn}_2\text{O}_7$.³⁶ This result further indicates that the two-magnon scattering plays a dominant role in both $\rho_{ab}(T)$ and $\rho_c(T)$ for $50 \leq T \leq 110$ K.

The field dependences of B_{ab}^{fit} and B_c^{fit} of $\text{La}_{1.2}\text{Sr}_{1.8}\text{Mn}_2\text{O}_7$ for $50 \leq T \leq 110$ K are shown in Figs. 4(a) and 4(b), respectively. Both B_{ab}^{fit} and B_c^{fit} are H dependent, implying a strong sensitivity of the two-magnon scattering to external fields, and saturate at high fields. The decrease of B_{ab}^{fit} and B_c^{fit} with increasing H is the source of the small negative magne-

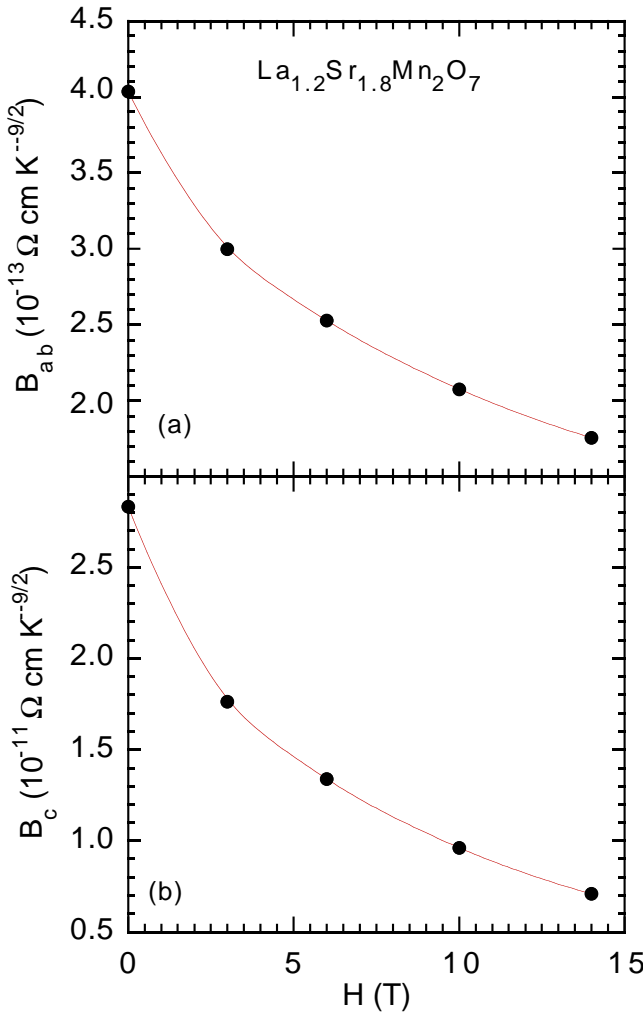


FIG. 4: Magnetic field H dependence of the coefficients (a) B_{ab} and (b) B_c of the $T^{9/2}$ functional dependence of the resistivities in the temperature range 50 to 110 K for $\text{La}_{1.2}\text{Sr}_{1.8}\text{Mn}_2\text{O}_7$. The lines are guides to the eyes.

toresistance for $50 \leq T \leq 110$ K. Their H dependence is also consistent with the spin wave scattering mechanism. Indeed, the spin-wave scattering itself should decrease with increasing H . The effect of an applied field is to open an energy gap $\Delta = g\mu(H + 4\pi M_s)$ in the magnon spectrum. This can be argued simply on the basis of a reduction in the spin-wave density by the applied field due to an increase in the energy gap appearing in the dispersion relation for the magnon energy, $\varepsilon_p = Dq^2 + \Delta$, where q is the magnon-wave vector.

Figures 5(a) and 5(b) are plots of $\sigma_{ab}(T)$ and $\sigma_c(T)$, respectively, of $\text{La}_{1.2}\text{Sr}_{1.8}\text{Mn}_2\text{O}_7$ in the low- T range, down to 1.9 K, measured in $H = 0$ and 14 T. Both σ_{ab} and σ_c follow a $T^{1/2}$ dependence below a certain T , which increases with increasing H . This is the first report of a $T^{1/2}$ dependence of σ_c of a bilayer manganite. The $T^{1/2}$ dependence of σ_{ab} is in agreement with previous reports

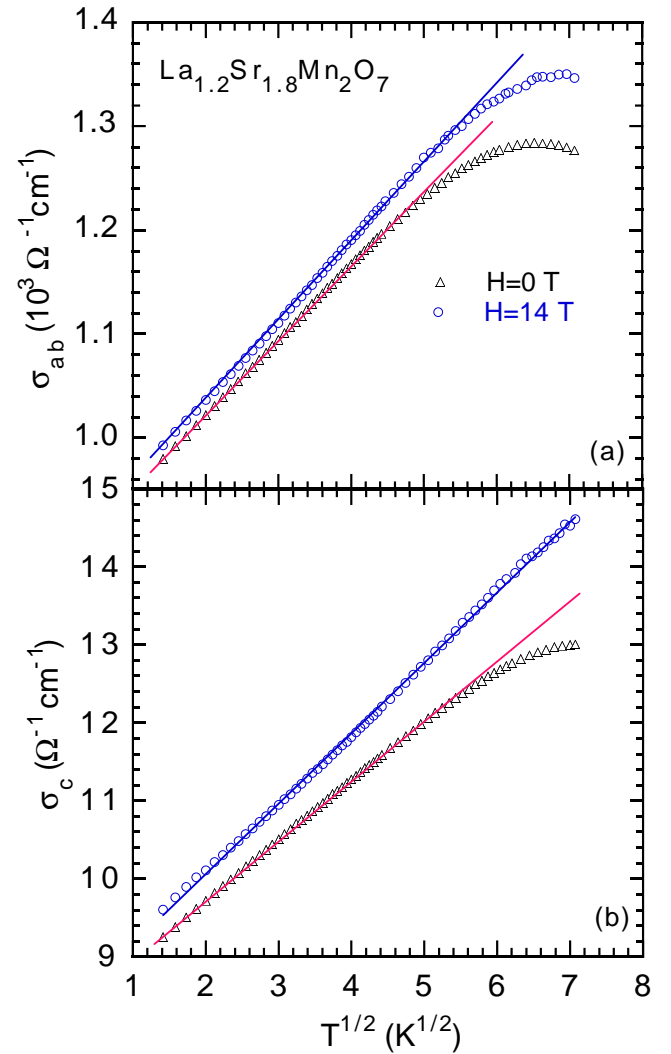


FIG. 5: (a) In-plane conductivity σ_{ab} and (b) out-of-plane conductivity σ_c vs $T^{1/2}$ for $\text{La}_{1.2}\text{Sr}_{1.8}\text{Mn}_2\text{O}_7$ measured down to 1.9 K and in applied magnetic fields $H = 0$ and 14 T.

both in $\text{La}_{1.2}\text{Sr}_{1.8}\text{Mn}_2\text{O}_7$ ¹⁴ and in $\text{La}_{1.3}\text{Sr}_{1.7}\text{Mn}_2\text{O}_7$ for $30 \text{ mK} \leq T \leq 2 \text{ K}$.¹⁶ It has been suggested¹⁶ that the observed $T^{1/2}$ dependence of σ_{ab} is consistent with weak localization effects in ordered 3D metals,^{37,38} where the density of states at the Fermi level has a $T^{1/2}$ singularity due to the influence of interference of the inelastic electron-electron interaction and the elastic impurity scattering of the electrons.³⁸ In the present case, the electrons are diffusive instead of freely propagating, leading to a profound modification of the traditional view based on the Fermi-liquid theory of metals. Considering the strong anisotropy of the crystal structure and of the conductivity, the bilayer manganites appear to be more 2D like. However, $\sigma_c(T)$ clearly follows the same $T^{1/2}$ dependence at low temperatures, consistent with 3D weak localization effects in disordered metals. This $T^{1/2}$ behavior in both $\sigma_{ab}(T)$ and $\sigma_c(T)$ confirms the 3D nature

of the metallic state and is in good agreement with the theory of quantum interference in highly anisotropic layered metals developed by Abrikosov.¹⁸

IV. CONCLUSION

We performed simultaneous in-plane and out-of-plane resistivity measurements on bilayer manganite $\text{La}_{1.2}\text{Sr}_{1.8}\text{Mn}_2\text{O}_7$ single crystal in magnetic fields applied parallel to the ab -plane. Both $\rho_{ab}(T)$ and $\rho_c(T)$ display a $T^{9/2}$ dependence for $50 \leq T \leq 110$ K. This T dependence and the magnitude of the fitting parameter are consistent with two-magnon scattering mechanism. The excellent agreement between the ratio of the exchange interactions J_{ab}/J_c obtained by fitting the data and that

deduced from neutron scattering provides further support for the validity of this scattering mechanism. Below 50 K, both $\sigma_{ab}(T)$ and $\sigma_c(T)$ follow a $T^{1/2}$ dependence, which is consistent with the theory of quantum interference or weak-localization effects in 3D disordered metals. The same temperature dependence for both conductivities strongly indicates that the bilayer $\text{La}_{1.2}\text{Sr}_{1.8}\text{Mn}_2\text{O}_7$ has a 3D metallic nature at $T < T_c$.

Acknowledgments

This research was supported at KSU by the National Science Foundation under Grant No. DMR-0102415. Work at LANL was performed under the auspices of the U. S. Department of Energy.

-
- ¹ P. Schiffer, A. P. Ramirez, W. Bao, and S.-W. Cheong, Phys. Rev. Lett. **75**, 3336 (1995).
- ² M. Jaime, P. Lin, M. B. Salamon, and P. D. Han, Phys. Rev. B **58**, R5901 (1998).
- ³ T. Okuda, A. Asamitsu, Y. Tomioka, T. Kimura, Y. Taguchi, and Y. Tokura, Phys. Rev. Lett. **81**, 3203 (1998).
- ⁴ T. Okuda, Y. Tomioka, A. Asamitsu, and Y. Tokura, Phys. Rev. B **61**, 8009 (2000).
- ⁵ G.-M. Zhao, V. Smolyaninova, W. Prellier, and H. Keller, Phys. Rev. Lett. **84**, 6086 (2000).
- ⁶ G.-M. Zhao, D. J. Kang, W. Prellier, M. Rajeswari, H. Keller, T. Venkatesan, and R. L. Greene, Phys. Rev. B **63**, R60402 (2000).
- ⁷ Y. Moritomo, A. Asamitsu, H. Kuwahara, and Y. Tokura, Nature (London) **380**, 141 (1996).
- ⁸ T. Kimura, Y. Tomioka, H. Kuwahara, A. Asamitsu, M. Tamura, and Y. Tokura, Science **274**, 1698 (1996).
- ⁹ T. G. Perring, G. Aeppli, Y. Moritomo, and Y. Tokura, Phys. Rev. Lett. **78**, 3197 (1997).
- ¹⁰ K. Hirota, Y. Moritomo, H. Fujioka, M. Kubota, H. Yoshizawa, and Y. Endoh, Jpn. J. Phys. Soc. **67**, 3380 (1998).
- ¹¹ M. Kubota, H. Fujioka, K. Ohoyama, K. Hirota, Y. Moritomo, H. Yoshizawa, and Y. Endoh, J. Phys. Chem. Solids, **60**, 1161 (1999).
- ¹² R. Osborn, S. Rosenbranz, D. N. Argyriou, L. Vasiliu-Doloc, J. W. Lynn, S. K. Sinha, J. F. Mitchell, K. E. Gray, and S. D. Bader, Phys. Rev. Lett. **81**, 3964 (1998).
- ¹³ Q. A. Li, K. E. Gray, and J. F. Mitchell, Phys. Rev. B **63**, 24417 (2000).
- ¹⁴ S. H. Chun, Y. Lyanda-Geller, M. B. Salamon, R. Suryanarayanan, G. Dhalenne, and A. Revcolevschi, cond-mat/0007249 (2000).
- ¹⁵ Q. A. Li, K. E. Gray, and J. F. Mitchell, Phys. Rev. B **59**, 9357 (1999).
- ¹⁶ T. Okuda, T. Kimura, and Y. Tokura, Phys. Rev. B **60**, 3370 (1999).
- ¹⁷ J. F. Mitchell, D. N. Argyriou, J. D. Jorgensen, D. G. Hinks, C. D. Potter, and S. D. Bader, Phys. Rev. B **55**, 63 (1997).
- ¹⁸ A. A. Abrikosov, Phys. Rev. B **61**, 7770 (2000).
- ¹⁹ N. O. Moreno, P. G. Pagliuso, C. Rettori, J. S. Gardner, J. L. Sarrao, J. D. Thompson, D. L. Huber, J. F. Mitchell, J. J. Martinez, and S. B. Oseroff, Phys. Rev. B **63**, 174413 (2001).
- ²⁰ C. N. Jiang, A. R. Baldwin, G. A. Levin, T. Stein, C. C. Almasan, D. A. Gajewski, S. H. Han, and M. B. Maple, Phys. Rev. B **55**, R3390 (1997).
- ²¹ G. A. Levin, T. Stein, C. C. Almasan, S. H. Han, D. A. Gajewski, and M. B. Maple, Phys. Rev. Lett. **80**, 841 (1998).
- ²² C. D. Potter, M. Swiatek, S. D. Bader, D. N. Argyriou, J. F. Mitchell, D. J. Miller, D. G. Hinks, and J. D. Jorgensen, Phys. Rev. B **57**, 72 (1998).
- ²³ S. B. Oseroff, N. O. Moreno, P. G. Pagliuso, C. Rettori, D. L. Huber, J. S. Gardner, J. L. Sarrao, J. D. Thompson, M. T. Causa, G. Alejandro, M. Tovar, and B. R. Alscio, J. Appl. Phys. **87**, 5810 (2000).
- ²⁴ B. Dabrowski, X. Xiong, Z. Bukowski, R. Dybzinski, P. W. Klamut, J. E. Siewenie, O. Chmaissem, J. Shaffer, C. W. Kimball, J. D. Jorgensen, and S. Short, Phys. Rev. B **60**, 7006 (1999).
- ²⁵ P. G. de Gennes, Phys. Rev. **118**, 141 (1960).
- ²⁶ T. Kasuya, Progr. Theor. Phys. (Kyoto) **22**, 227 (1959).
- ²⁷ D. A. Goodings, Phys. Rev. **132**, 542 (1963).
- ²⁸ A. S. Alexandrov and A. M. Bratkovsky, Phys. Rev. Lett. **82**, 141 (1999).
- ²⁹ D. B. Romero, V. B. Podobedov, A. Weber, J. P. Rice, J. F. Mitchell, R. P. Sharma, and H. D. Drew, Phys. Rev. B **58**, R14 737 (1998).
- ³⁰ L. Vasiliu-Doloc, S. Rosenkranz, R. Osborn, S. K. Sinha, J. W. Lynn, J. Mesot, O. H. Seeck, G. Preosti, A. J. Fedro, and J. F. Mitchell, Phys. Rev. Lett. **83**, 4393 (1999).
- ³¹ M. Matsukawa, H. Ogasawara, R. Sato, M. Yoshizawa, R. Suryanarayanan, G. Dhalenne, A. Revcolevschi, and K. Itoh, Phys. Rev. B **62**, 5327 (2000).
- ³² K. Kubo and N. Ohata, Jpn. J. Phys. Soc. **33**, 21 (1972).
- ³³ T. Chatterji, P. Thalmeier, G. J. McIntyre, R. van de Kamp, R. Suryanarayanan, G. Dhalenne, and A. Revcolevschi, Europhys. Lett. **46**, 801 (1999).
- ³⁴ H. Fujioka, M. Kubota, K. Hirota, H. Yoshizawa, Y. Moritomo, and Y. Endoh, J. Phys. Chem. Solids **60**, 1165 (1999).
- ³⁵ G. Khaliullin and R. Kilian, Phys. Rev. B **61**, 3494 (2000).
- ³⁶ T. Chatterji, L. P. Regnault, P. Thalmeier, R. Surya-

- narayanan, G. Dhalenne, and A. Revcolevschi, Phys. Rev. B **60**, R6965 (1999).
- ³⁷ P. A. Lee and T. V. Ramakrishnan, Rev. Mod. Phys. **57**, 287 (1985).
- ³⁸ B. L. Al'tshuler and A. G. Aronov, Zh. Eksp. Teor. Fiz. **77**, 2028 (1979) [Sov. Phys. JETP **50**, 968 (1979)].